Electronic Supplementary Information

Hydroxyapatite, an exceptional catalyst for the gas-phase deoxygenation of bio-oil by aldol condensation

Elodie G. Rodrigues, Tobias C. Keller, Sharon Mitchell and Javier Pérez-Ramírez*

Institute for Chemical and Bioengineering, Department of Chemistry and Applied Biosciences, ETH Zurich, Vladimir-Prelog-Weg 1, CH-8093 Zurich, Switzerland. Fax: +41 44 6331405 Tel: +41 44 6337120; E−mail: jpr@chem.ethz.ch.

Experimental section

Catalyst preparation

Calcium hydroxyapatites ($Ca_{10}(PO_4)_6(OH)_2$ in stoichiometric form) were precipitated by the dropwise addition of aqueous $(NH_4)_2HPO_4$ (0.40 mol L^{-1}, 98%, Sigma Aldrich) into a stirred aqueous solution of $Ca(NO_3)_2{\cdot}4H_2O$ (0.60 mol L^{-1}, 99%, Sigma Aldrich) at room temperature and constant pH (9.5), which was adjusted by the addition of ammonia solution (25%). The amount of $(NH_4)_2HPO_4$ was varied to yield nominal Ca/P ratios in the final solution of 1, 1.5, 1.64, 1.67, and 2. The resulting precipitate was stirred at the same temperature for 24 h, before it was isolated by filtration, thoroughly washed with deionised water, dried at 110ºC for 12 h, and finally calcined at 600ºC (heating rate 5ºC min^{-1}) for 2 h in static air to yield the fresh catalyst.

$Ca(OH)_2$ (96%, Sigma Aldrich) was calcined at 600ºC (heating rate of 5ºC min^{-1}) for 2 h under N_2 flow flow (50 cm^3 min^{-1}) to yield sample CaO. CsX was obtained by subjecting zeolite X (molar Si/Al ratio of 1.4, Sigma Aldrich) to 3 subsequent ion-exchange treatments in aqueous solutions of CsCl (0.1 mol L^{-1}, 8 h, 25ºC, 10 $g_{zeolite}$ L^{-1}). Mg-Al hydrotalcite (molar Mg/Al ratio = 3) was prepared by coprecipitation of an aqueous solution of $Mg(NO_3)_2{\cdot}6H_2O$ (0.75 mol L^{-1}, 99%, Fluka) and $Al(NO_3)_3{\cdot}9H_2O$ (0.25 mol L^{-1}, 99%, Acros) with a second solution of $NaOH/Na_2CO_3$ (2 mol L^{-1}) maintaining a constant pH of 10. The resulting precipitate was stirred at room temperature for 15 h, before it was isolated by filtration, thoroughly washed with deionised water, dried at 100ºC for 18 h, and calcined at 450ºC (heating rate of 5ºC min^{-1}) for 15 h in static air. This material was rehydrated in liquid-phase (1 h, 1 g of sample in 100 mL of water, 500 rpm) and finally re-calcined at 450ºC for 15 h to yield the activated catalyst (HT_a). Magnesium oxide nanopowder (high surface area, lot #A2592020) was purchased from Strem Chemicals.

Characterisation methods

The calcium and phosphorous contents in the solids were determined by inductively coupled plasma optical emission spectroscopy (ICP-OES) on a Horiba Ultima 2 instrument equipped with a photomultiplier tube detection. X-ray diffraction (XRD) patterns were measured on a PANalytical X'Pert PRO-MPD diffractometer using Ni-filtered Cu Kα radiation (λ = 0.1541 nm). Data were recorded in the 2θ range of

5-70° with an angular step size of 0.05° and a counting time of 8 s per step. X-ray photoelectron spectroscopy (XPS) was performed under ultra-high vacuum (10^{-9} mbar) using a Specs XPS spectrometer equipped with a high-intensity twin-anode (Al Kα radiation). Porous properties were determined by nitrogen sorption at -196ºC in a Micromeritics TriStar II instrument. Prior to the measurement, the samples were degassed in vacuum at 300ºC for 3 h. Mercury intrusion porosimetry was undertaken with a Micromeritics Autopore IV 9510 following *in situ* sample evacuation. Skeletal densities of the solids were measured by He pycnometry using a Micromeritics Accupyc II 1340 instrument. Prior to the analysis, the samples were dried in vacuum at 100ºC for 4 h. The values were determined by averaging 50 measurements collected after equilibration for 150 measurements. Energy dispersive X-ray (EDX) mapping was undertaken using a FEI Quanta 200F microscope operated at 20 kV. Scanning electron micrographs were acquired using a Zeiss Gemini 1530 FEG microscope (5 kV). Transmission electron microscopy and selected area electron diffraction was conducted on a FEI Tecnai F30 microscope (300 kV). Temperature-programmed desorption of carbon dioxide (CO_2-TPD) was carried out in a Micromeritics Autochem II chemisorption analyser equipped with a thermal conductivity detector and coupled with a MKS Cirrus 2 quadrupole mass spectrometer. The catalyst (0.1 g) was pre-treated in He flow (20 cm^3 min^{-1}) at 550ºC for 2 h. Afterwards, CO_2 (50 pulses, 1 cm^3) diluted in He flow (10 cm^3 min^{-1}) was adsorbed at 50ºC, followed by He purging at the same temperature for 60 min. CO_2 desorption was monitored in the range of 50-700ºC (heating rate of 10ºC min^{-1}). Temperature-programmed desorption of ammonia (NH_3-TPD) was carried out using the same equipment as for CO_2-TPD. After pre-treatment of the catalyst (0.1 g, 550ºC, 30 cm^3 min^{-1} He flow, 3 h), NH_3 (10 vol.% in 30 cm^3 min^{-1} He) was adsorbed in three sequential steps at 200ºC for 30 min, followed by He purging at the same temperature for 60 min. NH_3 desorption was subsequently monitored in the range of 200-700ºC (heating rate of 10ºC min^{-1}). Fourier transform infrared spectroscopy (FTIR) of pyridine was conducted in a Bruker IFS 66 spectrometer (650-4000 cm^{-1}, 2 cm^{-1} optical resolution, co-addition of 32 scans). Self-supporting wafers of catalyst (5 ton cm^{-2}, 30 mg, 1 cm^2) were degassed under vacuum (10^{-3} mbar) for 4 h at 420ºC, prior to adsorbing pyridine at room temperature. Gaseous and weakly adsorbed pyridine was subsequently removed by evacuation at different temperature (room temperature to 250ºC) for 30 min. The total concentration of Lewis (c_L) acid sites was calculated from the band area of adsorbed pyridine at 1445 cm^{-1}, using a previously determined extinction coefficient of $\varepsilon(L) = 2.94$ cm μmol^{-1} (C.A. Emeis, *J. Catal.*, 1993, **141**, 347). *In situ* Diffuse Reflectance Infrared Fourier Tranform (DRIFT) spectroscopy was performed using a Bruker Optics Vertex 70 spectrometer equipped with a high-temperature cell (Harrick) and a MCT detector. The samples were dried at 500ºC under N_2 flow for 2 h, then cooled to 50ºC prior to introducing CO_2 at this temperature. Spectra (4000-400 cm^{-1}, 4 cm^{-1} optical resolution, co-addition of 200 scans) were recorded at regular intervals between 50ºC and 400ºC under N_2 flow. Thermogravimetric analysis (TGA) of the catalysts after use in the aldol condensation of propanal was carried out with a Mettler-Toledo TGA/DSC 1 instrument. In a typical measurement, the used catalyst (15 mg) was heated from 25-900ºC in flowing air (60 cm^3 min^{-1}) with a ramp of 10ºC min^{-1}.

Catalytic tests

Experiments were carried out at atmospheric pressure in a continuous-flow fixed-bed reactor (12 mm internal diameter). The catalyst (0.1 g, particle size: 0.2-0.4 mm) was pretreated in He (50 cm^3 min^{-1}) at 450ºC for 1 h prior to the reaction. Propanal (99%, Acros Organics) was fed to the tubular reactor using a Chemyx Fusion 100 Classic syringe pump (1.2 cm^3 h^{-1}) *via* a vaporisation line (150ºC) and diluted with He (50 cm^3 min^{-1}). The reactions were conducted at 400ºC for 2-15 h and the educts were analysed by an on-line HP Agilent 6890 gas chromatograph equipped with a flame ionisation detector (FID) and a capillary HP-5 column. Conversion (X) and product yields (Y) were calculated based on the integrated peak area of the component of interest, normalised to the total FID response.

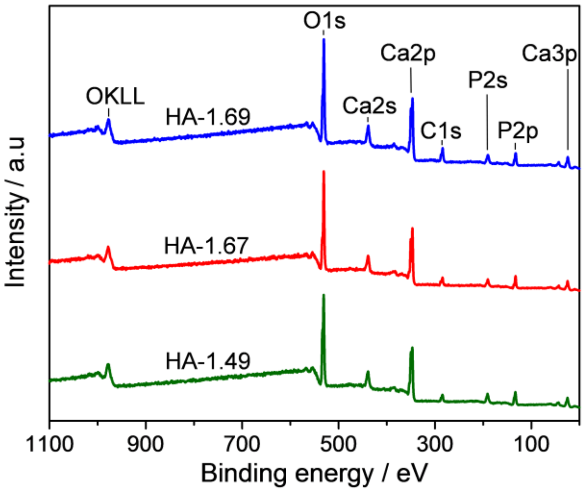

Fig. S1 X-ray photoelectron spectra (survey scan) of the hydroxyapatite catalysts.

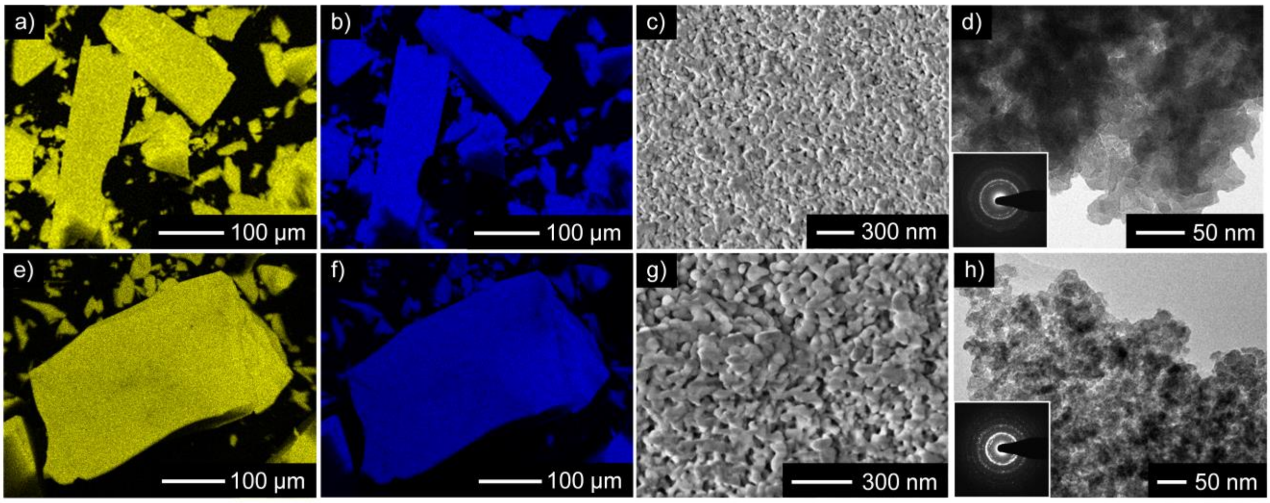

Fig. S2 EDX maps evidencing the macroscopic distributions of calcium (a) and phosphorus (b), SEM (c) and TEM (d) images of the particle and crystal morphology, and selected area electron diffraction pattern (d, inset) for the Ca-deficient HA-1.49. Equivalent analysis for the Ca-rich HA-1.69 (e-h).

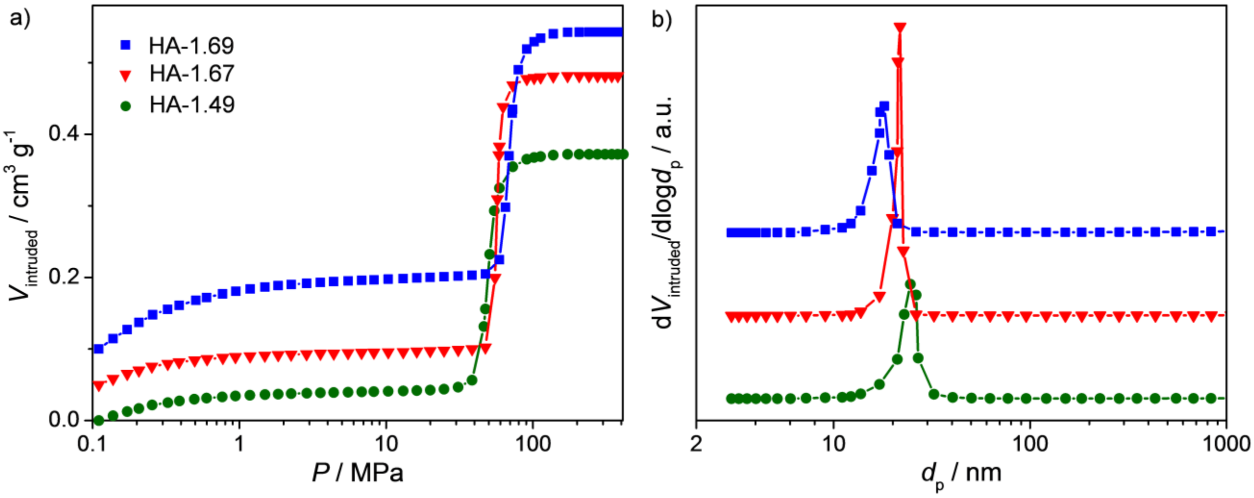

Fig. S3 Hg intrusion curves (0.05 cm^3 g^{-1} offset) (a) and pore size distributions (b) of the hydroxyapatite catalysts.

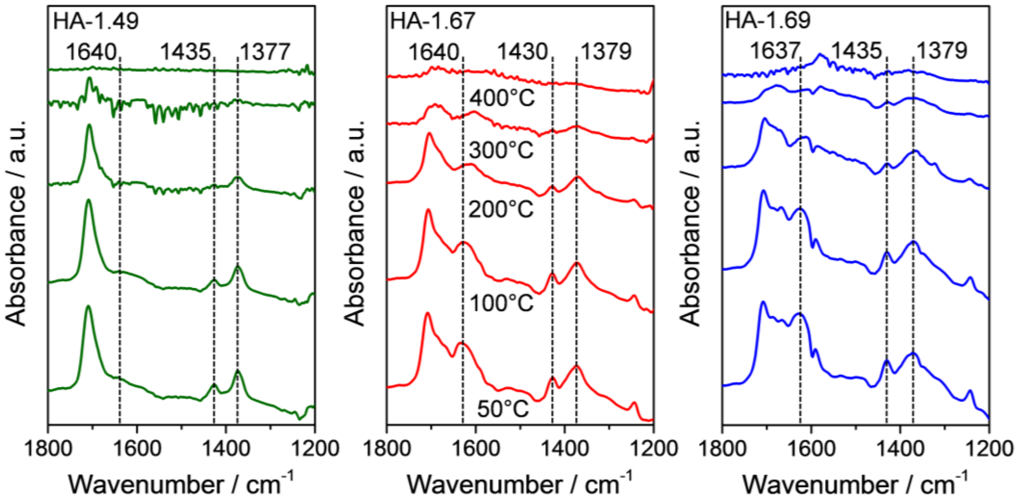

Fig. S4 DRIFT spectra of adsorbed CO_2 on the hydroxyapatite catalysts at different temperatures. The bands around 1380 and 1430 cm^{-1} are assigned to the formation of (PO_x)-carbonate species and carbonates at OH^- sites, respectively. The band around 1640 cm^{-1} corresponds to the formation of water ($CO_2 + 2\ OH^- \rightarrow CO_3^{2-} + H_2O$), whereas the multiplicity of contributions in the 1760-1590 cm^{-1} range is attributed to hydrogenocarbonate species HCO_3^-.

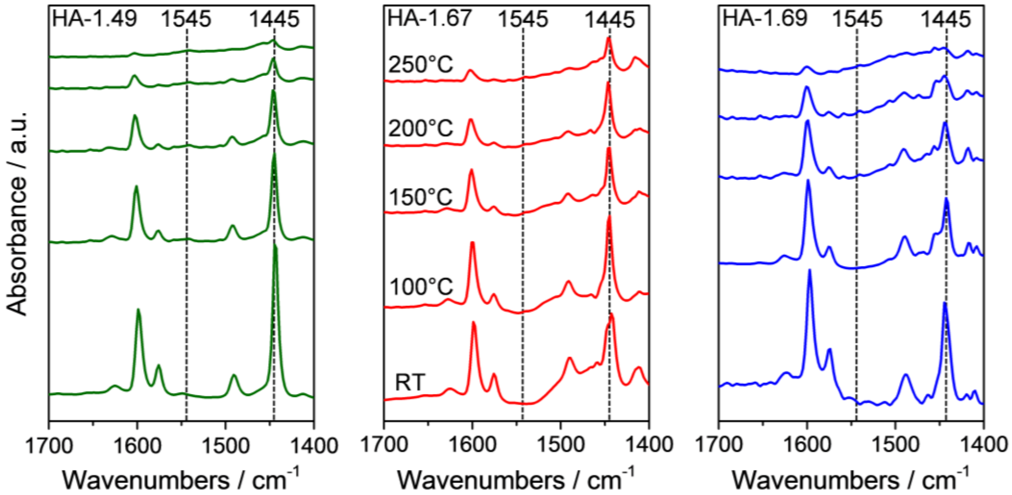

Fig. S5 FTIR spectra of adsorbed pyridine on hydroxyapatite catalysts at different temperatures. The appearance of a band characteristic of pyridine coordinated to Lewis acid sites (1445 cm^{-1}) and the absence of a corresponding band associated with Brønsted acid sites (1545 cm^{-1}) confirms the purely Lewis-type acidity of the HAs.

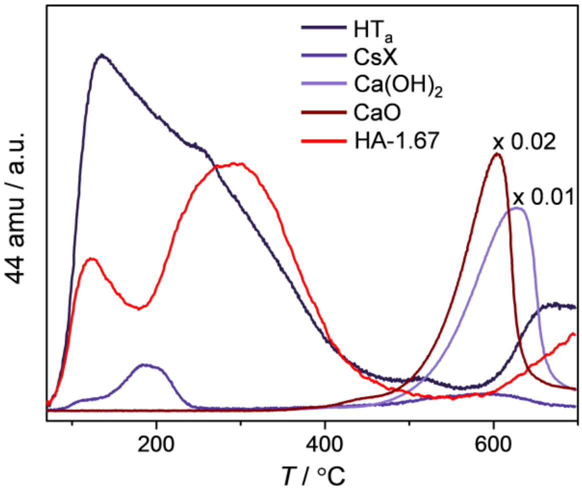

Fig. S6 CO$_2$-TPD profiles of the stoichiometric HA and benchmark base catalysts. The profiles were normalised to the specific surface area of the material.

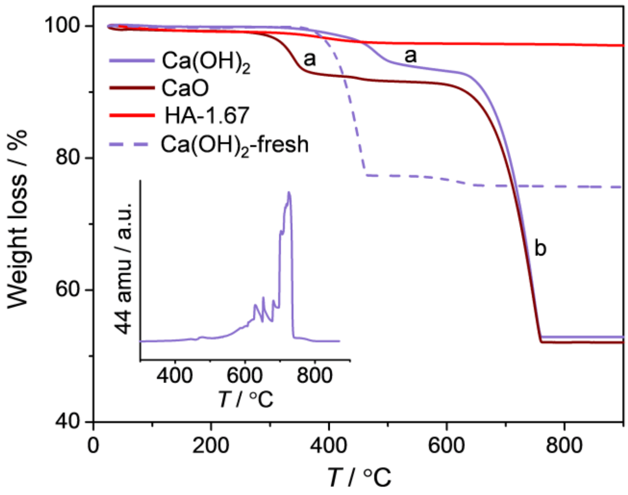

Fig. S7 Thermogravimetric profiles of selected catalysts after use in the aldol condensation of propanal for 2 h. Step (a) is tentatively ascribed to the decomposition of possible bicarbonate species formed at the surface during the reaction and (b) the evolution of CO_2 from the decomposition of $CaCO_3$ formed by the bulk carbonation of CaO during the reaction. The corresponding evolution of CO_2 observed over the $Ca(OH)_2$ catalyst after use (inset) is shown for reference.

Table S1 Initial product selectivity over the benchmark catalysts.

Catalyst	S_{dimer}	S_{trimer}
MgO_{nano}	78	10
HT_a	67	15
CsX	65	11

Reaction conditions: 0.1 g catalyst, 400ºC, WHSV = 9.72 h^{-1}, 50 cm^3 min^{-1} He flow.